scientific reports

Check for updates

OPEN

Sulfonohydrazide as a potential inhibitor of SARS-CoV-2 infection

Zoha Khan[1,2], Saba Farooq[1,2]✉, Atia-tul-Wahab[2], Hana'a Iqbal[1,2], Farzana Naz[3], Thomas Iftner[4], Khalid M. Khan[3], Muhammad Yusuf[5] & M. Iqbal Choudhary[1,2,3,6]✉

The COVID-19 pandemic caused immense mortality and morbidity reporting 704,753,890 cases worldwide. The repercussions of this pandemic are still being felt in the form of newly evolving variants and infections. The pandemic has pointed towards the need for the development of new and effective agents against SARS-CoV-2 infection. Sulfonohydrazides are a class of compounds with a wide range of therapeutic potential. The present study aims to identify the anti-SARS-CoV-2 potential of Sulfonohydrazide compounds. Twenty-five Sulfonohydrazides derivatives were evaluated for anti-viral potential *via* plaque reduction assay (PRA) and cytopathic effect (CPE) analysis *in-vitro*. Treatment point assay was employed for the strategic evaluation of antiviral compound at the particular stages of the SARS-CoV-2 life cycle. Gene expression analysis was also carried out, which was supported by immunofluorescence assays targeting the N and S proteins of SARS-CoV-2, alongside fold-change analysis, to identify a robust and multifaceted approach for the understanding of viral dynamics. Moreover, ligand-inhibitor interactions were assessed by *in- silico* studies. Compound 24 (4(*E*)-4-methyl-*N'*-(2,3,4-trihydroxybenzylidene)benzenesulfonohydrazide) was identified as the most potent molecule that inhibited SARS-CoV-2 infection (92.85 ± 3.57%) *via* PRA. The time point assay revealed that the effect of the compound might be at the entry point, which might be due to the down-regulation of the Spike (*S*) and Angiotensin-converting enzyme 2 (*ACE-2*) genes by the compound. The gene expression analysis of *ORF1a/b* by qRT-PCR indicated reduction in viral load after compound treatment, as indicated by a higher cycle threshold (Ct) value. Moreover, the compound 24 also downregulated the expression of *S*, *RdRp*, and *ACE-2*. Furthermore, the interaction of compound 24 with *S*, *RdRp*, and *ACE-2* was predicted *via* molecular docking, which validated the interaction and possible anti-SARS-CoV-2 effect. Additionally, immunofluorescence staining analysis of spike and nucleocapsid proteins also showed downregulation in SARS-CoV-2 infected cells. Overall, the acquired data suggested that Sulfonohydrazide derivative 24 inhibits SARS-CoV-2 entry and replication.

Keywords Severe acute respiratory syndrome coronavirus 2, Sulfonohydrazides, Antivirals, Multi-target therapeutics, Spike, RNA dependent RNA polymerase, Angiotensin-converting enzyme 2

Abbreviations

RDV	Remdisivir
S	Spike
N	Nucleocapsid
RdRp	RNA-dependent RNA polymerase
ACE-2	Angiotensin-converting enzyme 2
hpi	Hours post-infection
dpi	Days post-infection
qRT-PCR	Quantitative real-time–polymerase chain reaction
PRA	Plaque reduction assay
CPE	Cytopathic effect

[1]National Institute of Virology, Dr. Panjwani Centre for Molecular Medicine and Drug Research, International Center for Chemical and Biological Sciences, University of Karachi, Karachi 75270, Pakistan. [2]Dr. Panjwani Centre for Molecular Medicine and Drug Research, International Center for Chemical and Biological Sciences, University of Karachi, Karachi 75270, Pakistan. [3]H.E.J. Research Institute of Chemistry, International Center for Chemical and Biological Sciences, University of Karachi, Karachi 75270, Pakistan. [4]Institute for Medical Virology and Epidemiology of Viral Diseases, University Hospital and Medical Faculty, Eberhard Karls University, 72076 Tuebingen, Germany. [5]Department of Chemistry, Faculty of Mathematics and Natural Sciences, Universitas Padjadjaran, Jl Ir. Soekarno KM 21, Jatinangor 45363, West Java, Indonesia. [6]Department of Biochemistry, Faculty of Science, King Abdulaziz University, Jeddah 21412, Saudi Arabia. ✉email: sabafarooq000@yahoo.com; iqbal.choudhary@iccs.edu

Severe acute respiratory syndrome coronavirus 2 (SARS-CoV-2) is a Coronavirus (CoVs) and belongs to the family *Coronaviridae*, which primarily cause infections of the respiratory and gastrointestinal tracts[1]. In the late 2019, SARS-CoV-2 emerged as a highly transmissible and pathogenic virus causing a deadly pandemic of COVID-19 by early 2020 worldwide[2]. Like other RNA viruses, SARS-CoV-2 is prone to genetic alterations and rapidly adapt to new human host[3]. These viral genome mutations have resulted in the emergence of new variants with increased replicative fitness, altered pathogenicity, or differences in their ability to evade adaptive immune responses and resist antiviral drugs[4].

Clinical manifestations of COVID-19 can be asymptomatic or symptomatic and, in severe cases, fatal[5]. The immunopathology of each patient varies according to their common health status[6–8]. Currently, many different anti-viral therapeutic options are available against COVID-19 such as paxlovid (Nirmatrelvir + Ritonavir)[9], repurposed antiviral drugs (e.g., molnupiravir and remdesivir)[10], and monoclonal antibodies (e.g., adintrevimab)[11]. However, new SARS-CoV-2 variants have been emerging frequently, and there is no curative regimen yet available to tackle the infection and symptoms effectively. Therefore, identifying new and effective inhibitors of SARS-CoV-2, covering a wide range of variants, is crucial.

Hydrazides are organic compounds with diverse pharmacological and biological properties, such as antimicrobial, antiviral, antiparasitic, antifungal, anti-inflammatory, analgesic, and anticancer activities. Different functional groups in each compound give it unique characteristics[12]. A study has indicated that a series of synthetic α-aminophosphonate-hydrazone derivatives have antiviral activity with 65.1% curative, 74.3% protective, and 94.3% inactivation activities[13]. In a study, two compounds derived from benzylidene hydrazides were found to be active against Vesicular stomatitis virus (VSV) in HeLa cell cultures[14]. A study has reported anti-hepatitis C activity of diflunisal hydrazide-hydrazones. These have also been observed to show hepatocellular carcinoma inhibition[15]. A tecovirimat analogue, *p*-Trifluoromethylbenzohydrazide (spirovirimat) has shown potent antiviral activity against Monkeypox virus by abolishing extracellular virus production. In silico evaluation suggested that the derivative targets the same protein as the tecovirimat[16]. In a research evaluating a series of novel aryl benzoyl hydrazide analogs, some of the derivatives demonstrated potent inhibitory activity against the avian H5N1 flu strain. One of these analogs, even exhibited nanomolar antiviral effects against both the H5N1 and Flu B virus. Primary mechanistic studies proposed that these derivatives act by mainly interacting with the PB1 subunit of RNA-dependent RNA polymerase (RdRp)[17]. In a study, a synthesized hydrazide-containing oseltamivir analog demonstrated strong inhibition of neuraminidases from H5N1, H1N1, H5N1–H274Y, and H1N1–H274Y mutants[18]. In a molecular docking study, the binding affinity of a newly synthesized hydrazide derivative (E)-N'-(1-(4-bromophenyl)ethylidene)-2-(6-methoxynaphthalen-2-yl)propanehydrazide for the SARS-CoV-2 main protease enzyme was observed and intermolecular binding interactions were studied. The compound showed a stable binding mode at the enzyme active pocket with a binding energy value of -8.1 kcal/mol. Moreover, the enzyme-compound complex showed stable dynamics with highly favorable binding energies. Overall, the compound might be a good lead for further structural optimization against the main protease enzyme[19]. Another in silico study has explored a complex compound containing hydrazone-derived ligand-protein, which has shown potential to be antiviral drug in cervical cancer caused by HPV-18 (human papillomavirus)[20]. Therefore, these compounds could possibly have anti-SARS-CoV-2 potential can be investigated to be developed into antivirals agents. This present study is aimed at investigating the anti-SARS-CoV-2 activity of a Sulfonohydrazide derivative in vitro. The non-cytotoxic compounds were evaluated for their effects on viral and host gene, and protein expressions by qRT-PCR and immunofluorescence microscopy, respectively, to evaluate their antiviral potential. Out of 25 derivatives assessed, 11 non-cytotoxic compounds indicated moderate to high anti-SARS-CoV-2 activity (50–100% viral plaque reduction). The compound **24** was further assessed for its potential viral targets by time-point assay.

Results

Cytotoxicity and anti-SARS-CoV-2 activity of sulfonohydrazide derivatives

After screening of various classes of organic compounds, 25 Sulfonohydrazide derivatives were identified as potential inhibitors of SARS-CoV-2. Subsequently, their cytotoxicity profile and the antiviral potential were assessed (Supplementary Table-1). Remdesivir (RDV) was used as a positive control. The inhibitory effects of the compounds on the growth of Vero cells (ATCC-CCL-81) were assessed using an MTT assay. The most potent anti-SARS-CoV-2 effect was observed at the concentration of 83 µM. The cytotoxicity of 25 derivatives indicated that only 11 derivatives had < 20% cytotoxicity. Compound **24** indicated the highest viability/proliferation (> 90%), of Vero cells therefore, it was selected for subsequent assessments. The CPE reduction assay indicated consistent antiviral potential of compound **24**. IC_{50} of RDV and compound **24** were found to be 31.54 and 8.320 respectively while the CC_{50} values of RDV and compound **24** were 307.2 and 202.3, respectively (Fig. 1A,B).

The selectivity index (SI) of individual compound, is the ratio of 50% cytotoxicity concentration (CC_{50}) of normal kidney cells over IC_{50}, was also evaluated. SI represents the safety of testes compound relative to its anti-SARS-CoV-2 activity. The obtained results indicated that the compound 24 showed high selectivity index as compared to standard drug RDV (Table 1).

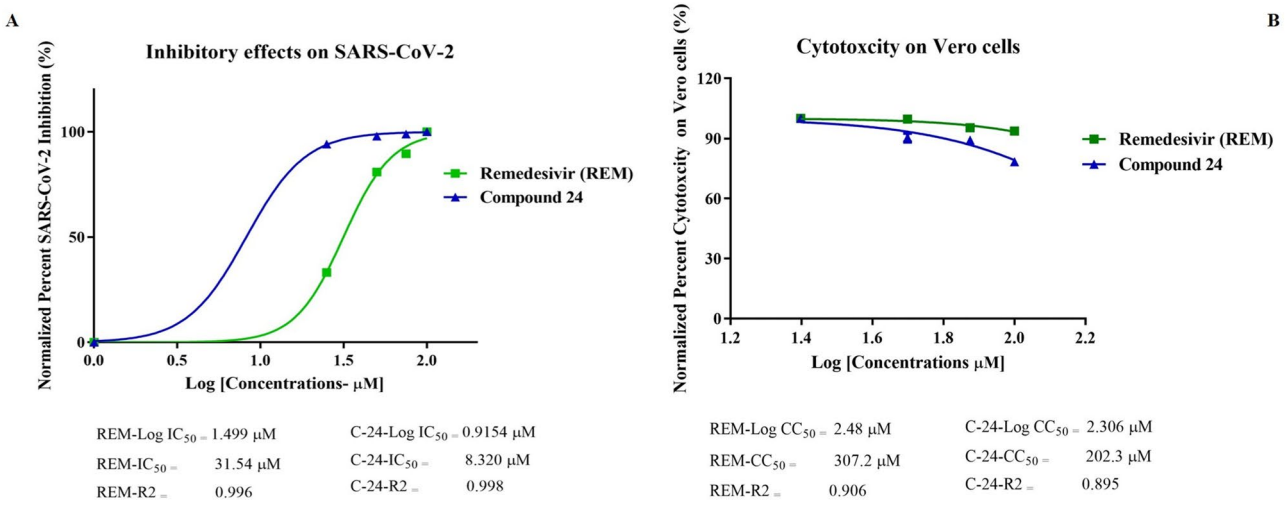

Fig. 1. The cytotoxicity profile and anti-SARS-CoV-2 potential of compound **24** and Remdesivir (RDV). (**A**) Represents the IC_{50} of compound **24** and RDV with the R^2 0.998 and 0.996, respectively; while (**B**) represents the CC_{50} of compound **24** and RDV with the R^2 0.895 and 0.906, respectively. The data is represented as mean ± SD.

S#	Compound/ IUPAC	CC_{50} (µM)	IC_{50} (µM)	SI (CC_{50}/ IC_{50})
1	Compound 24	202.3	8.320	24.31
2	Remdesivir	307.2	31.54	9.7

Table 1. The cytotoxic activity, antiviral activity, and selectivity indices of Compound 24.*SI* (Selectivity Index) = (CC_{50} Vero cell line/IC_{50} SARS-CoV-2 infected cell line). * Experiments were done in triplicate and repeated at least three times. The CC50 and IC50 values were calculated using nonlinear regression analysis of GraphPad Prism software (version 8) by plotting log inhibitor versus normalized response (variable slope).

Compound 24 inhibits cytopathic effects of SARS-CoV-2

The reduction of cytopathic effect of the compound and drugs was observed under a light microscope at 72 h post-infection (hpi), which indicated that compound **24** reduced > 90% of SARS-CoV-2 infection (Fig. 2). The potential of compound **24** to reduce the viral-induced CPE was further validated through a plaque reduction assay (PRA), which indicated that at the concentration of 83 µM compound **24** reduced plaque formation by 92.85 ± 3.57%. In contrast, plaque reduction by RDV was observed as 85.71 ± 5.45% (Fig. 2).

Effect of compound 24 at different time-points

To elucidate the possible viral entry or life cycle points (multi-target therapeutics) at which compound **24** acts to inhibit SARS-CoV-2, a time-point assay was carried out. The results indicated that compound **24** possesses strongest inhibitory effect at the "entry" time-point (2.17-fold inhibition), suggesting that it might inhibits SARS-CoV-2 entry into the cells. The assay also indicated towards prophylactic potential of the compound indicated by inhibition at this time point (0.8-fold inhibition). Additionally, the assay revealed that the compound also inhibits the post-entry stage, indicating its therapeutic potential (0.822-fold inhibition) (Fig. 3). A p-value < 0.001 with a R^2-score of 0.936 indicated the significance of the results and goodness-of-fit.

Potential gene targets of the compound 24

To further confirm the anti-SARS-CoV-2 activity of compound **24**, the effects of the compound **24** on expression of viral genes open reading frames 1a and 1b (*ORF1a/b*), nucleocapsid (*N*), spike (*S*), and RNA-dependent RNA polymerase (*RdRp*), and host cellular gene angiotensin-converting enzyme 2 (*ACE-2*) were assessed. The results indicated a significant decrease in the expression of *N* gene (fold-change = 0.29) by compound **24**, as compared to the RDV (p-value < 0.05) (Fig. 4). The compound treatment also significantly reduced the expression of the *S* gene (fold-change = 1.1), as compared to the RDV (p-value < 0.01). Furthermore, compound **24** caused highly significant (p-value < 0.001) down-regulation of the gene expressions of *ORF1a/b*, *ACE-2*, and *RdRp* with fold-changes of 2.05, 0.58, and 1.4, respectively (Fig. 4A–E) as compared to the drug control RDV.

Sulfonohydrazide derivative down-regulates the expression of SARS-CoV-2 spike and nucleocapsid proteins

In order to validate the gene expression studies, immunofluorescence assay of N and S proteins of SARS-CoV-2 in the infected Vero cells treated with the compound was carried out *via* fluorescence microscopic analysis

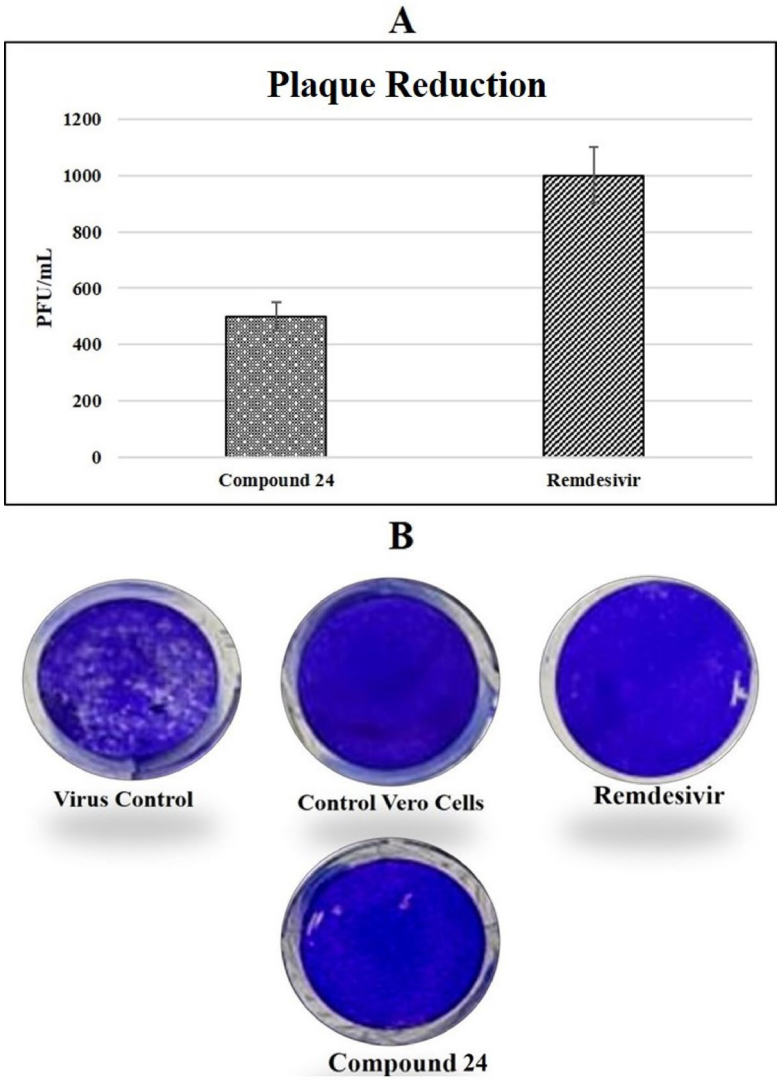

Fig. 2. Compound **24** efficiently reduced SARS-CoV-2-induced plaque formation. (**A**) A marked decrease in the PFU/mL was observed after treatment with compound **24** as compared to the Remdesivir at the concentration of 83 µM. (**B**) Representative images of Vero cells 5 dpi with SARS-CoV-2. Infected cells treated with compound **24** and RDV showed a lesser number of plaques than non-treated infected cells. The data is represented as mean ± SD.

(Fig. 5A,B). The results revealed that compound **24** reduced protein expression of S and N proteins as depicted by decreased fluorescent intensity (FI) of 1.34 and 0.88%, respectively as compared to the higher FI of 3.42 and 2.02% for S and N proteins, respectively in untreated virus-infected Vero control cells (Fig. 5C,D).

Protein-ligand docking indicated strong binding scores of the compound 24 with viral proteins

To assess how strongly compound **24** interacted with the Nucleocapsid-C terminal (NCT), Nucleocapsid-N terminal (NNT), S, ACE-2, and RdRp proteins, *in silico* molecular docking analysis was performed. Compound **24** interacted with ACE-2, S, NNT, NCT, and RdRp with the bond score of -5.242, -4.796, -5.778, -5.084, and − 5.375, respectively. Reported docking scores in general demonstrated that below − 6.0 kcal/mol are considered to indicate moderate binding, while scores below − 8.0 kcal/mol generally suggest strong binding and thus presented results indicate the moderate binding. Moreover, the hydrogen bond energies were − 2.09, -0.58, -3.77, -2.94, and − 0.49 (Fig. 6).

Discussion

In 2020, SARS-CoV-2 emergence brought a global pandemic with an unprecedented healthcare crisis[21], accounting for 775,335,916 confirmed cases and 7,045,569 deaths globally. In Pakistan, approximately 1,580,631 confirmed cases and 30,656 deaths were reported[22]. The loss in terms of morbidity, mortality, and economy worldwide that the pandemic has brought about has indicated the need of new and efficient antivirals. The

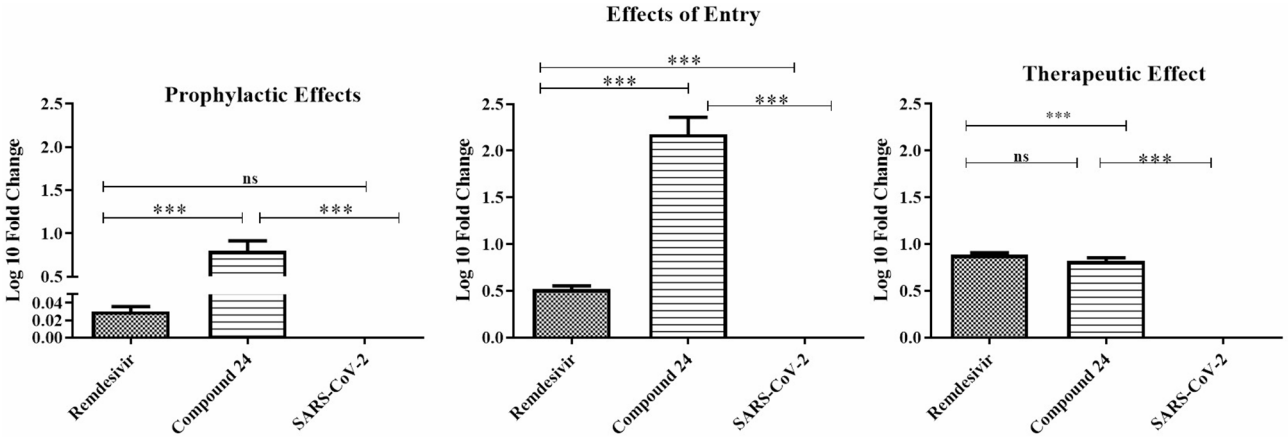

Fig. 3. Effect of compound **24** at different viral time points in compound-treated SARS-CoV-2 infected Vero cells. Log fold-change was calculated compared to virus-treated cells before (prophylactic), during (entry), and after (therapeutic) compound treatments at 83 µM concentration, and the mean fold-change was plotted. The asterisk indicates the significance between different groups. One-way ANOVA, followed by Bonferroni's Multiple Comparison Test was performed as a statistical analysis ($^{*}p < 0.05$, $^{**}p < 0.01$, $^{***}p < 0.001$).

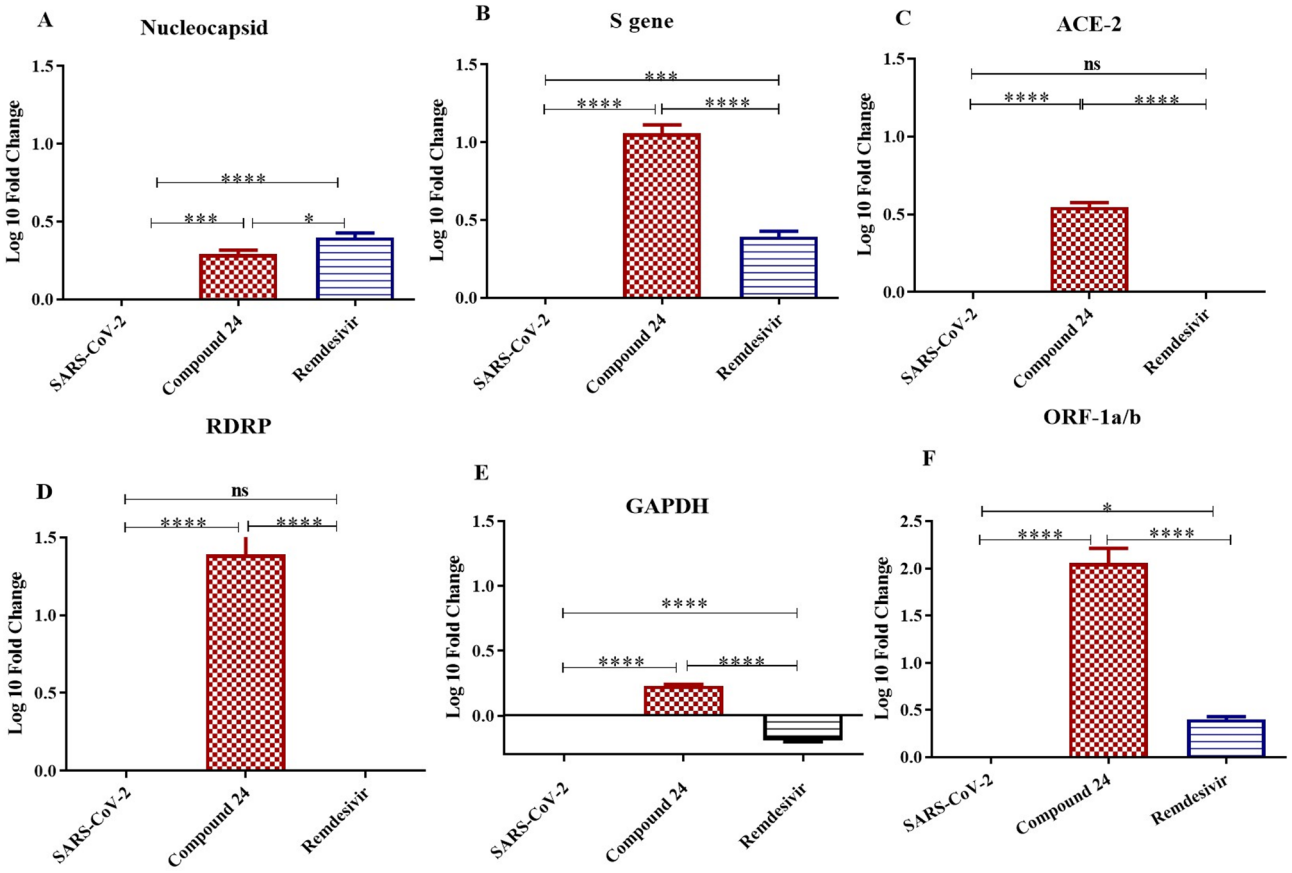

Fig. 4. Change in gene expression of (**A**) Nucleocapsid protein; (**B**) Spike protein; (**C**) ACE-2 receptor; (**D**) RNA-dependent RNA polymerase; (**E**) GAPDH; and (**F**) ORF1a/b, after compound **24** and drug treatments.

persistence of SARS-CoV-2 in the population long after the pandemic and emergence of new variants, points towards the necessity of developing better anti-SARS-CoV-2 agents. There is a need for potent anti-SARS-CoV-2 molecules that could inhibit the emerging variants. This study investigates the anti-SARS-CoV-2 potential of a series of Sulfonohydrazide derivatives on Vero cells. Out of the evaluated 14 Sulfonohydrazide derivatives, compound **24** was observed to have the standard drug-comparable cytotoxicity and the highest antiviral

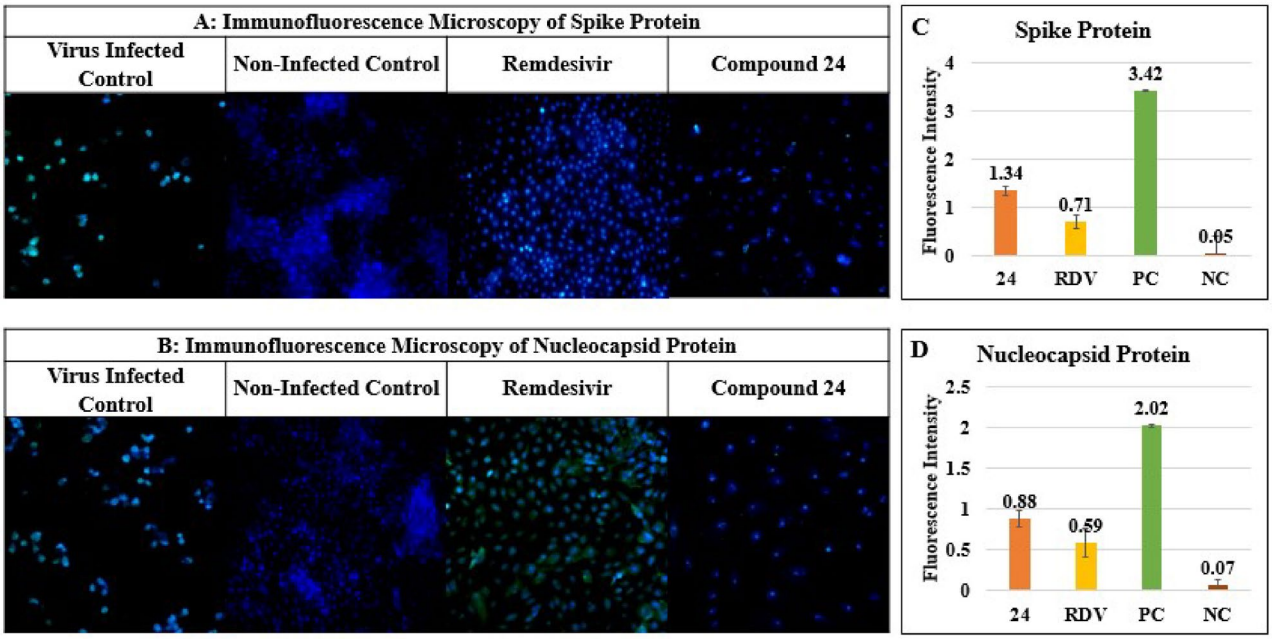

Fig. 5. The effect of compound **24** on the expression of SARS-CoV-2 S- and N-proteins. Representative immunofluorescence microscopic images of (**A**) Spike, and (**B**) Nucleocapsid proteins. Histograms of fluorescence intensity of (**C**) Spike, and (**D**) Nucleocapsid protein expressions using ImageJ software. RDV = Remdesivir, Blue fluorescence indicates the nucleus, and green fluorescence illustrates S or N protein.

effects. In vitro SARS-CoV-2 infection in Vero cells was confirmed by assessing cytopathic effects (CPE). Virus binding with cellular receptors consequently leads to viral tropism and pathogenicity by viral genomic RNA replication[23,24], which causes structural, metabolic, or functional alterations in the infected cell, this phenomenon is known as cytopathic effects (CPE)[24–26]. In our study, CPE analysis revealed that the monolayer of Vero cells was completely disrupted in non-treated virus-infected control cells; however, it was intact in the compound **24** and RDV treated cells. Furthermore, the number of morphologically healthy cells was higher in compound-treated infected cells as compared to that in the standard drug control. Consistent with the CPE assay, plaque reduction assay (PRA) also indicated that the infection was alleviated in compound-treated cells with a 92.85% infectivity reduction, as compared to RDV-treated infected cells (85.71%). The study demonstrated that the number of plaques in the compound-treated infected cells (5×10^2 PFU/mL) was reduced as compared to the RDV-treated infected cells (1×10^3 PFU/mL), indicating the potent effects of compound **24** in reducing viral load, replication, and infection as compared to the standard drug.

To assess the possible molecular targets of the compound **24** conducive to its antiviral potential, viral load after compound treatment was assessed at three-time points: (1) before the SARS-CoV-2 infection, to determine if a compound can be used as a prophylactic agent treatment, (2) during the infection, that is at the viral entry point, and (3) after the infection, to identify if the compound target viral replication cycle and could be used as a therapeutic agent against the infection. The efficacies of compound **24** and RDV were evaluated by quantifying viral copy numbers *via* qRT-PCR. The time-point assay revealed that compound **24** inhibited viral infection at all the three points; however, it demonstrated marked inhibition of viral entry, suggesting that it might suppress SARS-CoV-2 infection *via* ACE-2 receptor on the cell. Moreover, the data suggested that RDV had therapeutic potential, consistent with the previously reported studies, suggesting that RDV operates at the post-viral entry stage by targeting the replication cycle[27,28], validating our data.

To evaluate the gene targets through which compound **24** might act as a potential anti-SARS-CoV-2 gene expression analysis of viral genes including *Orf1a/b*, *N*, *S*, *RdRP*, and host receptor *ACE-2* was performed by qRT-PCR. *Orf1a/b* encodes ~ 70% of the SARS-CoV-2 genome[29,30]. It was observed that the compound significantly down-regulated the *Orf1a/b* gene with the fold change (FC) of 2.05 in comparison with the positive control (FC = 0.4) (p-value < 0.001), suggesting anti-SARS-CoV-2 activity of the compound.

The gene expression analysis revealed that compound **24** highly significantly down-regulated *S*-gene (p-value < 0.01) and very highly significantly downregulated the *ACE-2* gene (p-value < 0.001) expressions, validating that the compound controls the infection by targeting the SARS-CoV-2 entrance *via* S or ACE-2 proteins as observed in the time point assay. ACE-2 is a cellular membrane protein that has been shown to be implicated as a SARS-CoV-2 receptor in COVID-19 transmission and entry, thus is considered a competent target for viral inhibition. Several studies have revealed that reduced *ACE-2* expression can alleviate SARS-CoV-2 infection[31,32], whereas its upregulation enhances SARS-CoV-2 susceptibility[33]. Our data indicated that compound **24** could be used as a primary or secondary prophylaxis in COVID-19. Compound **24** also slightly reduced *N*-gene expression (p-value < 0.5). Moreover, *RdRp* expression analysis showed very highly significant

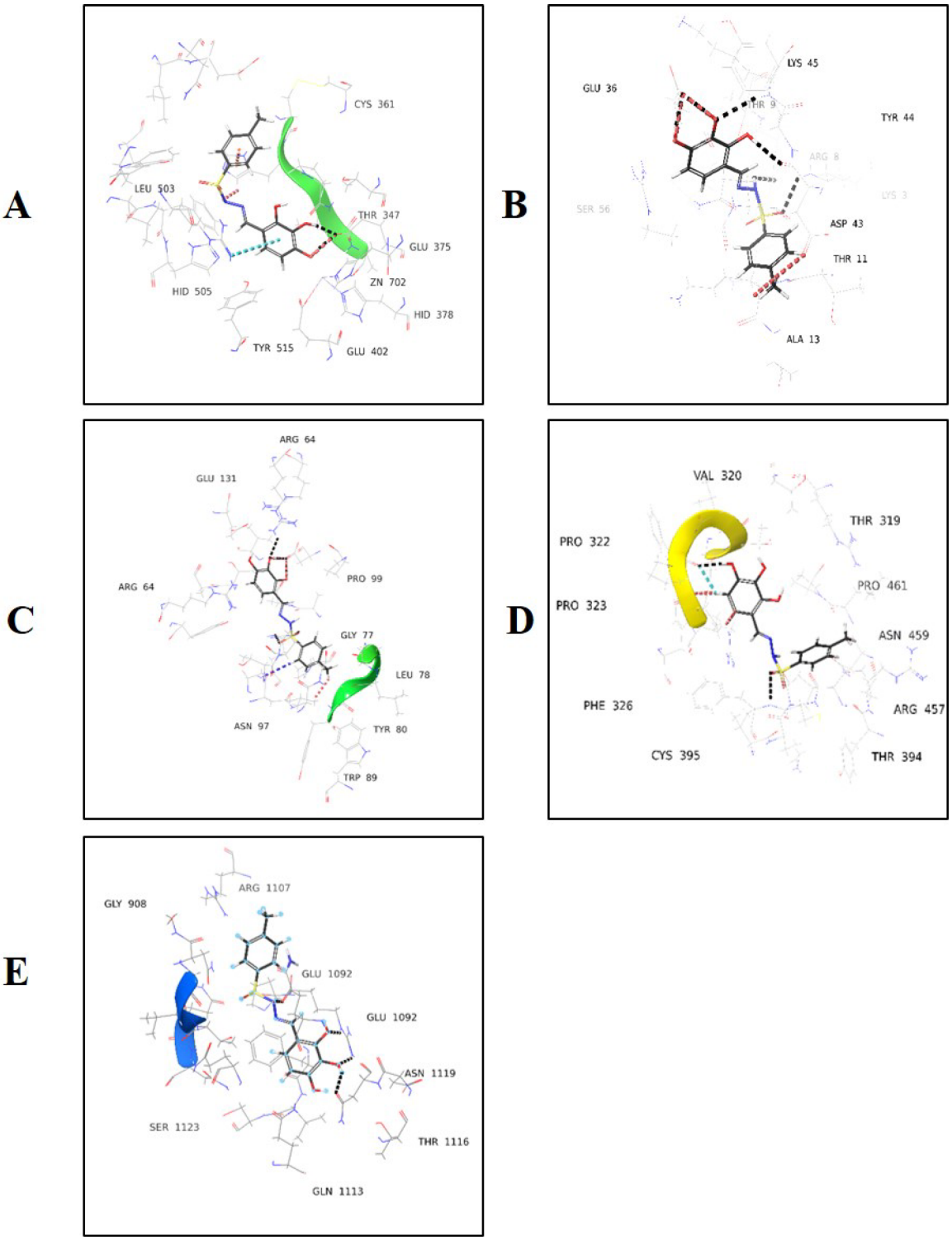

Fig. 6. Representative 3D images of ligand-protein profile. (**A**) ACE, (**B**) Nucleocapsid N-terminal (**C**) Nucleocapsid C-terminal, (**D**) RdRp, and (**E**) Spike proteins.

inhibition by compound **24** as compared to the RDV-treated infected cells (p-value < 0.001), indicating that compound **24** might also target viral replication, which is consistent with the observations of the time point assay. These data suggest that compound **24** might inhibit in-vitro SARS-CoV-2 infection by targeting *Orf1a/b*, *S*, *ACE-2*, and *RdRp* genes.

The effect of compound **24** at the protein level was determined *via* immunofluorescence microscopy at 72 hpi. Since the above data suggested that compound **24** inhibits viral entrance and replication, S and N proteins were selected as the protein analysis targets. Immunofluorescence microscopy presented a clear picture of the

SARS-CoV-2 infection of the Vero cells with or without treatment. The expression of both the S and N proteins in SARS-CoV-2-infected cells treated with compound **24** were observed to be reduced as compared to the untreated infected cells, indicating reduced protein expression. However, expression of both S and N proteins were higher for compound **24** treated infected group, as compared to the RDV-treated infected cells. Altogether, these observations indicate that compound **24** down-regulates S protein both at the genetic and protein levels, however, it is more potent at gene level when compared to the RDV-treated infected cells.

During the study, the Sulfonohydrazide derived compound **24**, was further analyzed in silico molecular docking to elucidate the possible interaction sites of S, nucleocapsid-C terminal domain (N-CTD), N-terminal domain (N-NTD), RdRp, and ACE-2 proteins with the potential inhibitor[33–37]. In silico results revealed that NCT and NNT binding scores (BS) of the compound were − 5.084 and − 5.778, respectively (PDB ID: 7U0N and 7CE0, respectively). It was also demonstrated that OH at the C21 and C22 positions of the compound **24** interacted with N-CTD *via* hydrogen (H) bond at LYS45, ASP43, and GLU36 with H-bond energy (HE) = -2.94. Furthermore, the O at C9 and C10 of compound **24** formed an H-bond with ARG106, and OH at C21 interacted with ASP101 of N-NTD (HE = -3.77). When the compound was docked with RdRp protein (PDB ID: 7CDZ), it revealed that C20 and C9 of compound **24** formed H-bond with PHE321 and PHE396 of RdRp, respectively (BS = -5.375, HE= -0.49). Docking with ACE-2 protein (PDB ID: 7bW4) indicated that GLU375 of ACE-2 interacted with OH at C22 of compound **24**, and a Pi-cation bond was also observed between ARG273 of ACE-2 protein and **24** (BS= -5.242, HE= -2.09). Moreover, in silico data also indicated that the NH group at C11 and OH at C21 of compound **24** interacted with GLU1092 and ARG1091 of S-protein *via* H-bond, respectively (BS = -4.796, HB = -2.09).

The findings of this study demonstrates the effects of Sulfonohydrazide derived compound **24** on SARS-CoV-2 entry, replication, and transcription as depicted by the downregulation of the *Orf1a/b*, *N*, *S*, *RdRp*, and *ACE-2* genes. This was validated by protein expression analysis showing reduced expression of N and S proteins in SARS-CoV-2 infected cells after compound treatment. The compound also inhibited the viral infection depicted by reduced CPE and plaque formation. Time-point assay suggested that the probably target of compound **24** is the viral entry validated by the down-regulation of *ACE-2* and *S* genes.

The current findings provide promising candidates for future drug development to fight against SARS-CoV-2, potentially targeting the COVID-19 pandemic and future viral threats. By identifying potent inhibitors, the research offers a foundation for subsequent investigations. However, there are some gaps particularly in terms of efficacy against emerging variant, and identification of potential effects in vivo studies. This work significantly contributes to the global health effort against COVID-19 and other viral pandemics. Future research should build on these results to bring this compound from the laboratory bench to the bedside, making them a potential tool in the global fight against infectious diseases.

Methodology

Compounds

The fully characterized and pure library of sylfonohdrazide derivatives were obtained from the Molecular Bank of PCMD, ICCBS, University of Karachi.

Cell lines

Vero cell line (ATCC CCL-81) was obtained from Bio-Bank, PCMD, ICCBS, University of Karachi and was grown as described previously[38]. Briefly, cells were cultured in Dulbecco's minimal essential medium, supplemented with 10% fetal bovine serum (FBS), 100 unit/mL penicillin, 100 µg/mL streptomycin, 1 mM sodium pyruvate and 4 mM L-glutamine and termed as complete media (cDMEM). To propagate SARS-CoV-2 virus, infection media (iDMEM) was prepared with Dulbecco's minimal essential medium, supplemented with 100 unit/mL penicillin, 100 µg/mL streptomycin, 1 mM sodium pyruvate and 4 mM L-glutamine.

Viral isolation and propagation

The SARS-CoV-2 wild-type strain was obtained from nasal swabs of COVID-19 patients and propagated in Vero cells as described by Case[39]. The virus was propagated by infecting Vero cells with 100 µL of viral transport medium (VTM) from the nasal swab in a tissue culture flask (25 cm^2) in infection media (iDMEM). After 5 days post-infection (dpi), supernatants were harvested and centrifuged at 2,000 rpm for 5 min to remove cell debris[40]. Viral load was determined by PCR, and upon confirmation, the samples were stored in sterile falcons at -80 °C for further experimentation. All experiments involving virus were performed in an approved BSL-III facility of the National Institute of Virology, Dr. Panjwani Center for Molecular Medicine and Drug Research (PCMD), International Center for Chemical and Biological Sciences (ICCBS), University of Karachi, Pakistan.

Cell viability assay

The cytotoxic effect of the compounds and RDV on Vero cells was identified by 3-(4,5-dimethylthiazol-2-yl)-2,5-diphenyltetrazolium bromide (MTT) assay[41]. Briefly, 2.5×10^4 cells/well were propagated in 96-well plates and incubated with the drugs and test compounds at 100, 75, 50, and 25 µM concentrations at 37 °C for 24 h. After incubation, MTT dye was added and was further incubated for 3–4 hours. Remdesivir was used as the positive control, untreated viral infected Vero cells were used as a negative control, and moreover DMSO control was also included in the study as a solvent control. All the experiments were performed in triplicates. After completion of the experiment, the absorbance was recorded by Multiskan Ascent Plate reader at 530 nm.

Cell viability (%)was measured as follows:

$$Cell\ viability\ (\%) = \left(\frac{OD\ of\ treated\ well - OD\ of\ untreated\ well}{OD\ of\ untreated\ well} \right) \times\ 100$$

The standard antiviral drug, RDV, demonstrated the highest SARS-CoV-2 reduction at a concentration of 83 µM. Based on the optimization of the drug at this concentration, compounds that showed minimal or no toxicity were further evaluated at this selected concentration. For the purpose of this study, 83 µM is considered the reference concentration or endpoint measurement. Furthermore, for the evaluation of safety of tested compounds, the ratio of the 50% cytotoxic concentration (CC_{50}) in normal kidney cells to the 50% inhibitory concentration (IC_{50}) in term of selectivity index (SI) was also evaluated.

Confirmation of viral propagation in vero cells via q-PCR

For the confirmation and further quantification of viral copy number, whole cellular RNA was isolated using the QIAamp Viral RNA Mini Kit (Qiagen, Germany). qPCR was performed by using Bosphore® Novel Coronavirus (2019-nCoV) Detection Kit v7 (Turkey) by following the manufacturer's protocol[42].

Viral cytopathic effect (CPE) assay

The cytopathic effects (CPE) of virus was evaluated by following the Reed–Muench method[40]. Briefly, 2.5×10^4 cells/well were propagated in a 96-well plate. After 24 h, cells were infected with the virus for 1 h at a MOI of 0.01. After 1 h, viral inoculate was removed, and cDMEM was added to each well with compound (83µM) or RDV. CPE was observed at 3 dpi, and scoring was performed based on cell viability under a light microscope. Images were captured to record cellular morphology and inhibitory effects of the compound.

Scoring:
1 = **0–25%** cell survival,
2 = **25-50%** viable cells,
3 = **50-75%** cells alive,
4 = **75-100%** of cells survived infection.

Virus titration and infectivity assay

The virus titration and infectivity assay was performed as described previously[43]. The Vero cells (1×10^5/well) were propagated in 24-well plate for 24 h, then infected with SARS-CoV-2 at a MOI of 0.01. After 1 h, cells were treated with the compound and RDV at 100, 75, 50, and 25 µM concentrations for 1 h. After incubation, Carboxymethyle cellulose (CMC) was overlaid, and the plate was incubated for 5 days. After 5 days, CMC was aspirated, and cells were fixed with 4% paraformaldehyde (PFA) and stained with 1% crystal violet. The viral plaques were counted and PFU/mL was calculated.

Time-point assays

For the prophylactic analysis, a previously described assay was performed[44]. Briefly, the Vero cells (ATCC-CCL-81) were pre-treated with the drugs or compound and cultured in an infection medium (iDEME) for 1 h, and the virus was introduced for 2 h to allow infection. Subsequently, the cells were washed twice with 1x PBS and incubated for 48 h in drugs dissolved in a fresh infection medium. For the effect of compound or drugs on viral entry, the Vero cells were treated with the drugs during the infection period (2 h), followed by the removal of the drug-virus mixture and cell washing. Subsequently, the cells were incubated in an infection medium without any treatment for 48 h. For the assessment of therapeutic effect, the Vero cells were first infected with the virus for 2 h, washed with 1x PBS, and then treated with drugs in a fresh infection medium for 48 h. For the quantification of viral copy number, RNA was extracted *via* the QIAamp Viral RNA Mini Kit (Qiagen, Germany) followed by q-PCR and log 10-fold change was calculated.

Immunocytochemistry

The Vero cells were plated in a 96-well plate at a cell density of 2.5×10^4 cells/well for immunofluorescence microscopy and incubated at 37 °C in 5% CO_2 for 5 days. At the end of 5 days, media was removed and the wells were washed with 1x PBS thrice. Following cell fixation with 4% PFA for 4 h, the cells were incubated with an optimized concentration of the spike (S) (MA5-35946, Invitrogen) and the nucleocapsid (N) (MAB10474, Invitrogen) monoclonal antibodies for 90 min, followed by 60 min of incubation with rabbit anti-mouse IgG FITC-linked secondary antibody. The cell nuclei were stained with DAPI for 15 min and the plate was observed under a fluorescence microscope (Nikon Eclipse). Representative images were captured at the magnification of 20x[45].

Gene expression analysis

The gene expression analysis was performed as previously described[46]. Total RNA was extracted using the QIAamp Viral RNA Mini Kit (Qiagen, Germany) as per the manufacturer's instructions. The expression of *S*, *N*, *RdRp*, and *ACE-2* genes was evaluated by real-time PCR. GAPDH was used as endogenous control. For *RdRp* and *ACE-2* gene analysis, each 10 µL reaction mixture comprised RT SYBR green PCR master mix, ddH2O, primer pairs, and cDNA template. For the gene expression analysis of *RdRp* and *ACE-2*, genes primers were obtained from Macrogen, Inc. The PCR conditions were: 95 °C for 3 min, 40 cycles of 95 °C for 10 s and (A) for 30 s, followed by 72 °C for 1 min and lastly, 72 °C for 5 min. Where A corresponds to an annealing temperature of 58 °C and 59.3 °C for *RdRp* and ACE-2, respectively. Melting curve analysis (65 °C for 5 s, and then 0.5 °C for 5 s until 95 °C) was performed after this reaction. For S and N gene expression analysis, the TaqPath COVID-19 Combo Kit (Applied Biosystems, Thermofisher Scientific) was utilized as per the kit's guide. Relative RNA

abundance was quantified by using the comparative CT (ΔΔCT) method and $\log_{10}$ fold-change was calculated. Briefly, the ΔCt was calculated for each sample and control, followed by difference in ΔCt of the sample and the control, which is known as ΔΔCT. In order to determine level of change in the expression of the target gene in the test sample differs from that in the control sample, fold-change was calculated by the following formula:

Fold Change = 2^(-ΔΔCT).

A $\log_{10}$ of the fold-change was calculated, which is interpreted as; positive $\log_{10}$ value indicates upregulation (fold change > 1), and a negative $\log_{10}$ value indicates downregulation (fold change < 1). If the fold change is 1 (no change), $\log_{10}(1) = 0$.

The primer sequences used were:

RdRp:

Forward: 5'-GTGARATGGTCATGTGTGGCGG-3'.

Reverse: 5'-CARATGTTAAASACACTATTAGCATA-3'.

ACE-2:

Forward: 5'-TCCAITGGTCTTCTGTCACCCG-3'.

Reverse: 5'-AGACCATCCACCTCCACTTCTC-3'.

Protein-ligand docking

The 3D crystallographic structure of S-protein, nucleocapsid-C terminal (NCT), nucleocapsid-*N*-terminal (NNT), RdRp, and ACE-2 were downloaded from the Protein Data Bank (PDB) database (PDB IDs: 7U0N, 7CE0, 7CDZ, and 7bW4). The Maestro software was employed to perform the protein-compound docking analysis[47]. The crystal structures were processed using the Protein Preparation Wizard. The compound's (ligands) structure was obtained from the molecular bank of the International Institute of Chemical and Biological Sciences and drawn using Chem3Draw Ultra 13.0. The compound was prepared using the LigPrep tool[21]. The site map tool was used to generate the top 5 ligand binding sites; the highest affinity site was selected for the grid generation *via* the Receptor Grid Generation tool. The Ligand Docking tool was employed for docking. The interactions between the ligand and receptor, such as hydrogen bonds and hydrophobic and electrostatic interaction, were determined using the Maestro graphical interface.

Statistical analysis

The data entry, analysis, and processing were performed using GraphPad Prism (Version 8.02). All results are expressed as the mean ± standard deviation (SD). The data was analyzed using One-way ANOVA, followed by Bonferroni's Multiple Comparison Test. The *p*-values less than 0.05 were designated as statistically significant for all results.

Conclusion

Our study provides evidence that studied Sulfonohydrazide derivative possess anti-SARS-CoV-2 properties. The study on compound **24** demonstrates that this molecule can efficiently alleviate the infection by targeting the cellular entrance of the SARS-CoV-2 viruses, and affecting overall replication or transcription by targeting *ORF1a/b*, *S*, *RdRp*, and *ACE-2*. The findings also suggest that compound **24** can serve as a potent drug molecule to treat COVID-19, and which can be developed as an anti-viral agent.

Data availability

All data generated or analyzed during this study are included in this published article.

Received: 5 December 2024; Accepted: 21 May 2025
Published online: 28 May 2025

References

1. Lamers, M. M. & Haagmans, B. L. SARS-CoV-2 pathogenesis. *Nat. Rev. Microbiol.* **20** (5), 270–284 (2022).
2. WHO. *Coronavirus disease (COVID-19) pandemic. World Health Organization*, Geneva. https://www.who.int/emergencies/diseases/novel-coronavirus-2019 (2020).
3. Sanjuán, R. & Domingo-Calap, P. Mechanisms of viral mutation. *Cell. Mol. Life Sci.* **73**, 4433–4448 (2016).
4. Cascella, M. et al. Features, evaluation, and treatment of coronavirus (COVID-19) [Updated 2023 Aug 18]. In: StatPearls [Internet]. Treasure Island (FL): StatPearls Publishing; Jan (2024).
5. Flerlage, T., Boyd, D. F., Meliopoulos, V., Thomas, P. G. & Schultz-Cherry, S. Influenza virus and SARS-CoV-2: pathogenesis and host responses in the respiratory tract. *Nat. Rev. Microbiol.* **19** (7), 425–441 (2021).
6. Zhou, X., Li, Y., Li, T. & Zhang, W. Follow-up of asymptomatic patients with SARS-CoV-2 infection. *Clin. Microbiol. Infect.* **26** (7), 957–959 (2020).
7. Azkur, A. K. et al. Immune response to SARS-CoV-2 and mechanisms of immunopathological changes in COVID-19. *Allergy* **75** (7), 1564–1581 (2020).
8. Sourij, C. et al. Humoral immune response to COVID-19 vaccination in diabetes is age-dependent but independent of type of diabetes and glycaemic control: the prospective COVAC-DM cohort study. *Diabetes Obesity Metab.* **24** (5), 849 – 58 . (2022).
9. Wen, W., Chen, C., Tang, J., Wang, C., Zhou, M., Cheng, Y., & Mao, Q. Efficacy and safety of three new oral antiviral treatment (molnupiravir, fluvoxamine and Paxlovid) for COVID-19: a meta-analysis. *Ann. Med.* **54** (1), 516–523 (2022).
10. Mule, S. et al. Drug repurposing strategies and key challenges for COVID-19 management. *J. Drug Target.* **30** (4), 413–429 (2022).
11. Schmidt, P., Narayan, K., Li, Y., Kaku, C. I., Brown, M. E., Champney, E., … Walker,L. M. Antibody-mediated protection against symptomatic COVID-19 can be achieved at low serum neutralizing titers. *Sci. Transl. Med.* **15** (688), eadg2783. (2023).
12. Verma, G. et al. M. A review exploring biological activities of hydrazones. *J. Pharm. Bioallied Sci.* **6** (2), 69 (2014).
13. Tian, J., Ji, R., Wang, H., Li, S. & Zhang, G. Discovery of novel α-aminophosphonates with hydrazone as potential antiviral agents combined with active fragment and molecular Docking. *Front. Chem.* **10**, 91145 (2022).
14. Kumar, D. et al. Benzylidene/2-chlorobenzylidene Hydrazides: synthesis, antimicrobial activity, QSAR studies and antiviral evaluation. *Eur. J. Med. Chem.* **45** (7), 2806–2816. https://doi.org/10.1016/j.ejmech.2010.03.002 (2010).

15. Şenkardes, S. et al. Synthesis of novel diflunisal hydrazide-hydrazones as anti-hepatitis C virus agents and hepatocellular carcinoma inhibitors. *Eur. J. Med. Chem.* **10**, 301–308. https://doi.org/10.1016/j.ejmech.2015.10.041 (2016).
16. Rossi, S. et al. Discovery of p-Trifluoromethylbenzohydrazide derivatives as potent antiviral agents against Monkeypox virus. *ACS Med. Chem. Lett.* https://doi.org/10.1021/acsmedchemlett.5c00075 (2025).
17. Liu, X. et al. Discovery of Aryl benzoyl Hydrazide derivatives as novel potent Broad-Spectrum inhibitors of influenza A virus RNA-Dependent RNA polymerase (RdRp). *J. Med. Chem.* **65** (5), 3814–3832. https://doi.org/10.1021/acs.jmedchem.1c01257 (2022).
18. Zhao, H. et al. Discovery of hydrazide-containing oseltamivir analogues as potent inhibitors of influenza A neuraminidase. *Eur. J. Med. Chem.* **221** https://doi.org/10.1016/j.ejmech.2021.113567 (2021).
19. Mohamed, S. K. et al. Synthesis, crystal structure, and a molecular modeling approach to identify effective antiviral Hydrazide derivative against the main protease of SARS-CoV-2. *J. Mol. Struct.* **1265**, 133391. https://doi.org/10.1016/j.molstruc.2022.133391 (2022).
20. Abidiy, S. I. et al. Antiviral activity of hydrazone derivatives based benzohydrazide/2-thiohydantoin analogs against HPV-18 (human papillomavirus): In silico study. *AIP Conf. Proc.* **3071** (1), 020015. https://doi.org/10.1063/5.0206875 (2024).
21. Ciotti, M. et al. The COVID-19 pandemic. *Crit. Rev. Clin. Lab. Sci.* **57** (6), 365–388 (2020).
22. WHO Coronavirus (COVID-19) Dashboard. World Health Organization. https://covid19.who.int/?adgroupsurvey={adgroupsurvey}&gclid=Cj0KCQjwhL6pBhDjARIsAGx8D58-_nkvD0e-LoIj0P-ZBF4C2ugQA_HXRtECt8OOCjCuToxfPkTAFf4aAtQhEALw_wcB. (2023).
23. V'kovski, P., Kratzel, A., Steiner, S., Stalder, H. & Thiel, V. Coronavirus biology and replication: implications for SARS-CoV-2. *Nat. Rev. Microbiol.* **19** (3), 155–170 (2021).
24. Oxford, A. E., Halla, F., Robertson, E. B. & Morrison, B. E. Endothelial cell contributions to COVID-19. *Pathogens* **9** (10), 785 (2020).
25. Lowenstein, C. J. & Solomon, S. D. Severe COVID-19 is a microvascular disease. *Circulation* **142** (17), 1609–1611 (2020).
26. Drożdżal, S. et al. J. FDA-approved drugs with pharmacotherapeutic potential for SARS-CoV-2 (COVID-19) therapy. *Drug Resist. Updates*. **53**, 100719 (2020).
27. Wang, M. et al. Remdesivir and chloroquine effectively inhibit the recently emerged novel coronavirus (2019-nCoV) *in vitro*. *Cell Res.* **30** (3), 269–271 (2020).
28. Nguyen, H. T., Falzarano, D., Gerdts, V. & Liu, Q. Construction of a noninfectious SARS-CoV-2 replicon for antiviral-drug testing and gene function studies. *J. Virol.* **95** (18), 10–128 (2021).
29. Helmy, Y. A. et al. The COVID-19 pandemic: a comprehensive review of taxonomy, genetics, epidemiology, diagnosis, treatment, and control. *J. Clin. Med.* **9**, 1225 (2020).
30. Arya, R. et al. Structural insights into SARS-CoV-2 proteins. *J. Mol. Biol.* **433**, 166725 (2021).
31. Brevini, T. et al. FXR Inhibition May protect from SARS-CoV-2 infection by reducing ACE-2. *Nature* **615**, 134–142 (2023).
32. Oh, C. K. et al. Targeted protein S-nitrosylation of ACE-2 inhibits SARS-CoV-2 infection. *Nat. Chem. Biol.* **19**, 275–283 (2023).
33. Garreta, E. et al. A diabetic milieu increases ACE-2 expression and cellular susceptibility to SARS-CoV-2 infections in human kidney organoids and patient cells. *Cell Metabol.* **34**, 857–873 (2022).
34. Peng, Y. et al. Structures of the SARS-CoV-2 nucleocapsid and their perspectives for drug design. *EMBO J.* **39**, e105938 (2020a).
35. Peng, Q. et al. Structural and biochemical characterization of the nsp12-nsp7-nsp8 core polymerase complex from SARS-CoV-2. *Cell Rep.* **31** (2020).
36. Xu, Y. et al. Off-target *in vitro* profiling demonstrates that Remdesivir is a highly selective antiviral agent. *Antimicrob. Agents Chemother.* **65**, 10–128 (2021).
37. Geng, Q. et al. Structural basis for human receptor recognition by SARS-CoV-2 Omicron variant BA.1. *J. Virol.* **96**, e00249–e00222 (2022).
38. Ogando, N. S. et al. J. T. J. O. G. V. SARS-coronavirus-2 replication in vero E6 cells: replication kinetics, rapid adaptation and cytopathology. **101** (9), 925 (2020).
39. Case, J. B., Bailey, A. L., Kim, A. S., Chen, R. E. & Diamond, M. S. Growth, detection, quantification, and inactivation of SARS-CoV-2. *Virology* **548**, 39–48. https://doi.org/10.1016/j.virol.2020.05.015 (2020).
40. Reed, L. J. & Muench, H. A simple method of estimating fifty-percent endpoints. *Am. J. Hyg.* **27**, 493–497 (1938).
41. Rekha, S. & Anila, E. I. *Vitro* cytotoxicity studies of surface modified CaS nanoparticles on L929 cell lines using MTT assay. *Mater. Lett.* **236**, 637–639 (2019).
42. Malik, H. et al. Identification of effective synthetic molecules against viral-induced cytokine release syndrome using in silico and in vitro approaches. *Mol. Diversity* 1–13. https://doi.org/10.1007/s11030-025-11136-3 (2025).
43. Farooq, S., Wahab, A. T., Rahman, A. U. & Choudhary, M. I. Preventive potential of dietary extracts against SARS-CoV-2 infections. *Curr. Traditional Med.* **10**, 31–39. https://doi.org/10.2174/2215083809666230116141143 (2024).
44. Fatima, R., Farooq, S., Moin, S. T., Choudhary, M. I. & Yousuf, S. Creating cocrystal salts: synthesis, crystal structure, Hirshfeld surface analysis and quantum chemical calculations of pyrimethamine and their potential anti- SARS-Cov-2 activity. *J. Mol. Struct.* **1325** https://doi.org/10.1016/j.molstruc.2024.140982 (2025).
45. Yang, J. et al. Fluorogenic reporter enables identification of compounds that inhibit SARS-CoV-2. *Nat. Microbiol.* **8**, 121–134. https://doi.org/10.1038/s41564-022-01288-5 (2023).
46. Khan, A. M., Wahab, A. T., Farooq, F., Ullah, A. & Choudhary Repurposing of US-FDA approved drugs against SARS-CoV-2 main protease (Mpro) by using STD-NMR spectroscopy, in Silico studies and antiviral assays. *Int. J. Biol. Macromol.* **234**, 123540 (2023).
47. Schrodinger *Maestro* https://www.schrodinger.com/products/maestro (2023).

Acknowledgements

The authors would like to acknowledge Prof. Dr. Daniel Sauter from the Institute for Medical Virology and Epidemiology of Viral Diseases, University Hospital and Medical Faculty, Eberhard Karls University, Tuebingen-72076, Germany, for his guidance in manuscript review.

Author contributions

Z.K.: performed the experiments and analysis, original draft writing, S.F.: supervision performed the formal analysis, designed the methodology, prepared, reviewed, and edited the manuscript. A-T.W.: Conceptualized and designed the study, managed the project, reviewed and edited the manuscript, and discussed the results critically; H.I.: reviewed and edited the manuscript and discussed the research and results. T.I.: Reviewed and edited the manuscript. K.M.K: Reviewed and edited the manuscript. FN: Compound Synthesis. M.Y.: Reviewed and edited the manuscript. M.I.C.: Provided the resources, conceptualization, managed the project, discussed the results critically, and reviewed and edited the manuscript. All authors approved the final version of the manuscript.

Funding

This research was conducted by the Institutional Recurring Research funds to Saba Farooq.

Declarations

Competing interests
The authors declare no competing interests.

Ethics approval and consent to participate
The research study was ethically approved by the Independent Ethics Committee (IEC), Dr. Panjwani Center for Molecular Medicine and & Drug Research, International Center for Chemical and Biological Sciences, University of Karachi (Reference # ICCBS/IEC-066-HNS/PC2021/Protocol/2.0). This study was conducted in accordance with the principles of the Declaration of Helsinki. All experiments were performed in accordance with relevant guidelines and regulations.

Consent to participate
Informed consent for taking the nasal swab have been obtained from participant in accordance with relevant guidelines and regulations.

Additional information
Supplementary Information The online version contains supplementary material available at https://doi.org/10.1038/s41598-025-03685-2.

Correspondence and requests for materials should be addressed to S.F. or M.I.C.

Reprints and permissions information is available at www.nature.com/reprints.

Publisher's note Springer Nature remains neutral with regard to jurisdictional claims in published maps and institutional affiliations.